

LS-65  
July 17, 1986

Comparison of LINDA and POISSON of a Dipole Field Calculation

S. H. Kim

Comparison of LINDA and POISSON of a Dipole Field Calculation

S. H. Kim

Two-dimensional magnetic field computations of a dipole magnet using LINDA and POISSON are compared. The purpose is not to distinguish the basic differences between the two codes, but to compare the results for different mesh sizes in a given problem region. The magnet geometry chosen for the calculation is the 6-GeV injector synchrotron H-type dipole magnet.

Figure 1 is the geometry used for LINDA runs. The outside air region is required to satisfy the geometrical constraints of the input parameters in LINDA. LINDA divides the problem space into uniform rectangular meshes. The maximum dimensions of the mesh outlay are 302 x 115. The plane,  $y = 0$ , in Fig. 1 is a flux normal boundary and the other three sides are flux parallel boundaries. The shim size is  $1.25/0.90$  cm x  $0.092$  cm as shown in Fig. 1.

The meshes and flux lines of a POISSON run are shown in Fig. 2. The outside air region in LINDA did not change the results in the POISSON run and were removed to reduce the number of meshes. In POISSON, the convergence criteria in the RMS sense is that the vector potential does not change by  $5 \times 10^{-7}$  at any mesh point. The corresponding RMS convergence criteria in LINDA is given as  $1 \times 10^{-7}$ .

In Fig. 3 relative field variations,  $\Delta B/B_o = (B-B_o)/B_o$ , along the symmetry plane from POISSON and LINDA runs are plotted. Here  $B_o$  is the field at  $(x,y) = (0,0)$ . The thickness of the shim is fixed as 0.92 mm. Only the mesh size, which is uniform over the problem space, is varied. From Fig. 3, curves #1 and #2 of POISSON and curves #3 and #4 of LINDA, it appears that calculations with smaller mesh sizes show the presence of the shim better than those with larger meshes. At the same time, for a given mesh size, it appears that LINDA sees the shim better than POISSON. Curves #6 and #7 are between

curves #4 and #2. It is not clear whether the result is converging between #4 and #2. It is assumed here that curves #5, #8, and #9, which have a mesh dimension of 0.5 cm in one or both directions, are less reliable data compared to the others in the figure. This is from the assumption that calculations with smaller mesh sizes should be more reliable than those with larger mesh sizes.

After increasing the shim thickness from 0.92 mm to 0.98 mm, the field was calculated again. The LINDA calculations are shown in Fig. 4. Except curve #5 of 0.5 cm x 0.5 cm mesh, there is a tendency for  $\Delta B/B_0$  to have higher values for curves with smaller mesh sizes.

In Fig. 5, POISSON runs of two different kinds of meshes are plotted. It is seen from curves #1, #2, #4, and #5, that calculations with equal weight triangle meshes respond to the shim better than those with right triangles. Also, runs with smaller meshes have larger values of  $\Delta B/B_0$  than those with larger meshes.

For the same shim thickness of 0.98 mm, if one compares POISSON and LINDA runs of Fig. 5, #1 and #2, and Fig. 4, #2 and #4, it appears again that LINDA sees the shim better than POISSON.

When the thickness of the shim is increased from 0.92 mm to 0.98 mm, it is interesting to note that the increase of  $\Delta B/B_0$  near  $x = 1.5$  cm, for example, is approximately  $0.6 \times 10^{-4}$  for both POISSON and LINDA runs with different mesh sizes of 0.25 cm x 0.25 cm and 0.125 cm x 0.125 cm. This is seen by comparing Fig. 3, #1 and #2 and Fig. 5, #2 and #1 for POISSON, and by comparing Fig. 3, #3 and #4 and Fig. 4, #4 and #2 for LINDA.

Figure 6 compares LINDA and POISSON calculations for the two different B-H tables shown in Tables 1 and 2. The Fermilab B-H Table has a higher B/H ratio compared to the POISSON B-H Table except at two values of  $B = 16.5$  kG and 18.0 kG. As shown in Fig. 6, runs using the Fermilab B-H Table for both the codes show higher  $\Delta B/B_0$  than those used with the POISSON B-H Table. Since the flux density in the shim is slightly higher than other iron areas, this may be another reason why LINDA responds to the shim better than POISSON.

As mentioned earlier, only uniform rectangular meshes over the problem space are allowed in LINDA. In POISSON, on the other hand, uniform or non-uniform triangular meshes are allowed. Tables 3 and 4 compare the POISSON calculations of 0.125 cm x 0.125 cm uniform meshes except near the shim, and 0.125 cm ~ 0.5 cm non-uniform meshes. The non-uniform meshes near the coil region are shown in Fig. 7. From Tables 3 and 4, it is seen that the difference of the magnetic field at the origin is  $\Delta B/B_o = 0.25 \times 10^{-4}$  and the relative variations of the two runs for  $x < 2.5$  cm is less than  $10^{-6}$ .

POISSON calculates the higher harmonics of the magnetic field at a normalized radius  $R$ . Then, the field at any point,  $z = x + iy$ , is given by

$$B_x - iB_y = \sum_{N=1}^{\infty} \left( -\frac{N \cdot B_N}{R} + i\frac{N \cdot A_N}{R} \right) (z/R)^{N-1}. \quad (1)$$

The above harmonic decomposition in a dipole field can also be expressed

$$B_y + iB_x = B_o \sum_{n=1}^{\infty} (b_n + ia_n) (x + iy)^n, \quad (2)$$

or  $B_y = B_o \left[ 1 + \sum_{n=1}^{\infty} r^n (b_n \cos n\theta - a_n \sin n\theta) \right],$

$$B_x = B_o \sum_{n=1}^{\infty} r^n (a_n \cos n\theta + b_n \sin n\theta).$$

In the symmetric midplane of  $y = 0$ ,

$$\begin{aligned} B_y(x) &= B_o \sum_{n=0}^{\infty} b_n x^n, \\ B_x(x) &= B_o \sum_{n=1}^{\infty} a_n x^n, \end{aligned} \quad (3)$$

where  $b_n$  and  $a_n$  are normal and skew coefficients of  $2(n+1)$  - poles.

In Table 5(a), the harmonic analysis coefficients,  $N \cdot A_N / R$  and  $b_n$ , of Eqs. (1) and (3) are shown for the case of 0.125 cm x 0.125 cm uniform meshes (see Table 3, Fig. 5, #1). As shown in Fig. 5, #1,  $\Delta B/B_o$  at  $x = 1.75$  cm is  $\sim 0.8 \times$

$10^{-4}$ . Table 5(b) for the case of  $0.125 \text{ cm} \sim 0.5 \text{ cm}$  non-uniform meshes, and Table 5(a) agree quite well for sextupole ( $N = 3$ ,  $n = 2$ ) and decapole ( $N = 5$ ,  $n = 4$ ) coefficients. The coefficients of higher poles start to deviate from each other. This seems to be reasonable if one compares Tables 3 and 4.

In order to compare the field calculations for different mesh distortions near the shim, the shim region could be distorted by considering the shim as a separate iron region or as a part of the whole iron region. The mesh distortions of the two cases near the shim are shown in Fig. 8. The magnetic fields of the two cases are shown in Tables 6 and 7. The differences,  $\Delta B/B$ , between the two tables are less than  $1 \times 10^{-6}$ . Table 8 shows the coefficients of the harmonic analysis of the two runs. They agree up to 22th-pole ( $N = 11$ ,  $n = 10$ ) quite well.

To compare the above real problem with a perfect case, a perfect dipole magnet was calculated using POISSON. The present version of LINDA, however, allows only limited geometries as shown in Fig. 9, and does not allow a perfect dipole field geometry. Figure 10 shows the perfect dipole geometry used for POISSON. In Fig. 10(a), the area corresponding to the shim is air, but the meshes are distorted similar to the real geometry. The magnetic field calculation with distorted meshes and one with uniform meshes are compared in Tables 9 and 10. In both cases,  $\Delta B/B_0$  is  $\sim \pm 0.2 \times 10^{-4}$  and the mesh distortion did not change the degree of random variations of  $\Delta B/B_0$ .

The harmonic analysis of the uniform and distorted meshes are compared in Table 11. It is seen from the table that when the coefficients  $N A_N/R$  are on the order or less than  $10^{-3}$  ( $b_n \sim 10^{-7}$ ), the coefficients do not agree with each other.

The following conclusions could be made from the preceeding discussions of a dipole magnet. Similar comparisons may be necessary for a quadrupole magnet.

- (1) For a given mesh size in a reasonable range, it appears that LINDA sees the shim better than POISSON (Or LINDA over-responds to the shim). A LINDA calculation with  $0.25 \text{ cm} \times 0.25 \text{ cm}$  meshes, for example, is between

two POISSON calculations with  $0.25 \text{ cm} \times 0.25 \text{ cm}$  and  $0.125 \text{ cm} \times 0.125 \text{ cm}$  meshes.

- (2) Even with the same mesh size, calculations of the two codes gives only differences of  $\Delta B/B_0 < 0.2 \times 10^{-4}$  for  $x < 1.75 \text{ cm}$ .
- (3) For both LINDA and POISSON, calculations with smaller mesh sizes have higher values of  $\Delta B/B_0$ .
- (4) Variations of  $\Delta B/B_0$  due to the change of the shim thickness seem to be the same for LINDA and POISSON. This seems to be in conflict with conclusion (1).
- (5) In POISSON, calculations with equal weight triangle meshes respond to the shim better than those with right triangle meshes.
- (6) In both LINDA and POISSON, calculations with Fermilab B-H table give slightly higher values of  $\Delta B/B_0 (\sim 0.1 \times 10^{-4})$  than those with the POISSON B-H table.
- (7) In POISSON, one can get reasonable results for a reduced number of meshes (case of non-uniform distribution of the meshes) and from distorted meshes in the shim region.
- (8) The accuracy of the harmonic coefficients in POISSON seems to be limited to  $N \cdot A_n/R > 10^{-3}$  ( $b_n > 10^{-7}$ ). (The magnitudes of the coefficients depend on the aperture. Therefore, this accuracy limit is not in an absolute sense).

SK:er

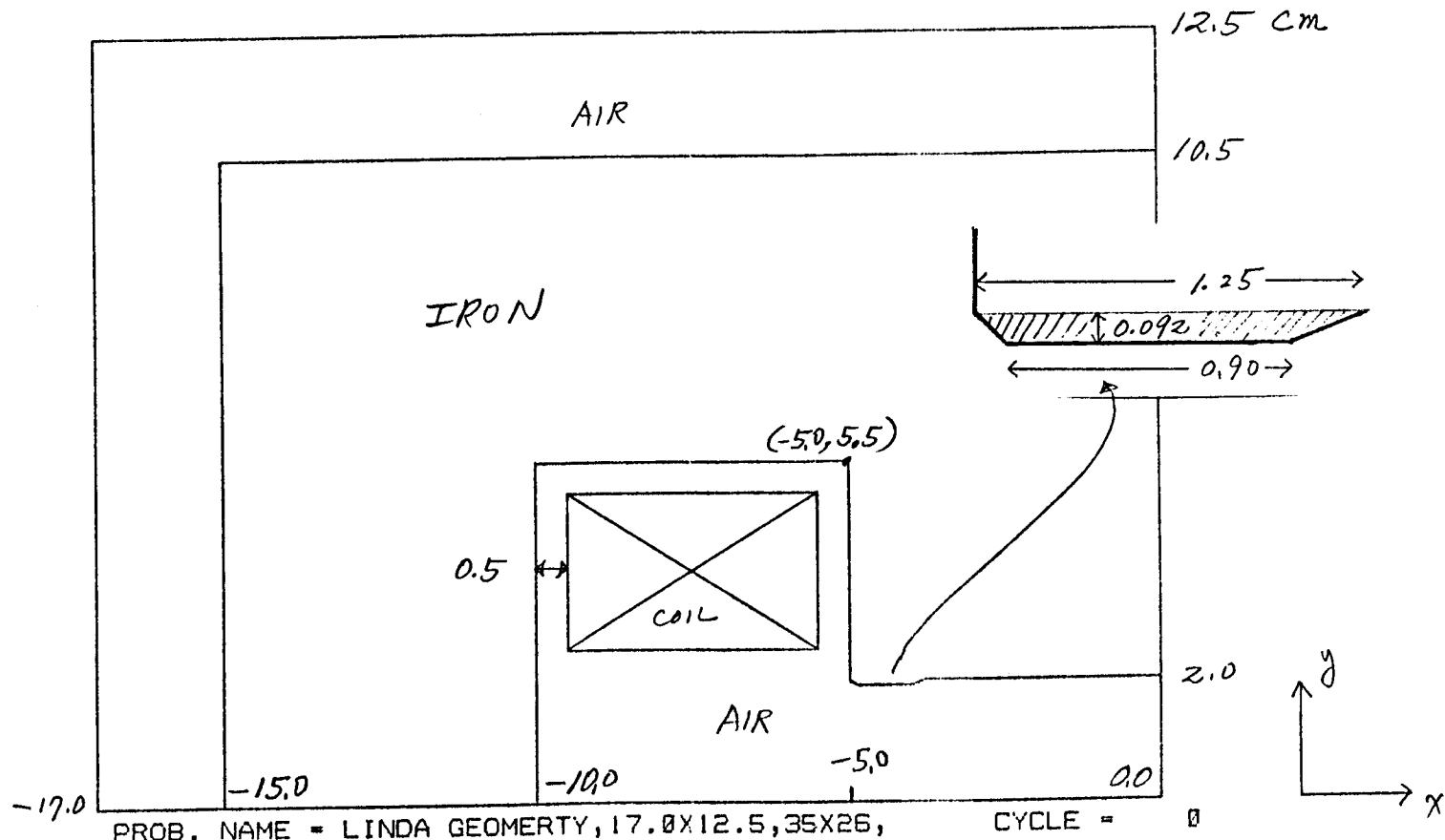


Fig. 1. Magnet geometry used for LINDA run.  $y = 0$  plane is the flux normal boundary. The outside air region is required in LINDA.  
 (Quadrant 2 of 1/2 symmetrical H-magnet)

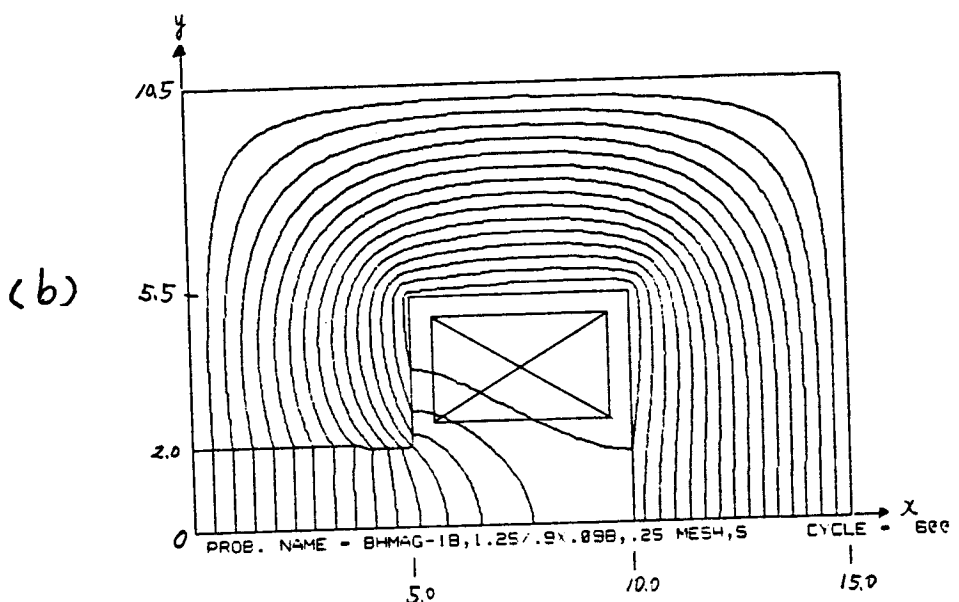
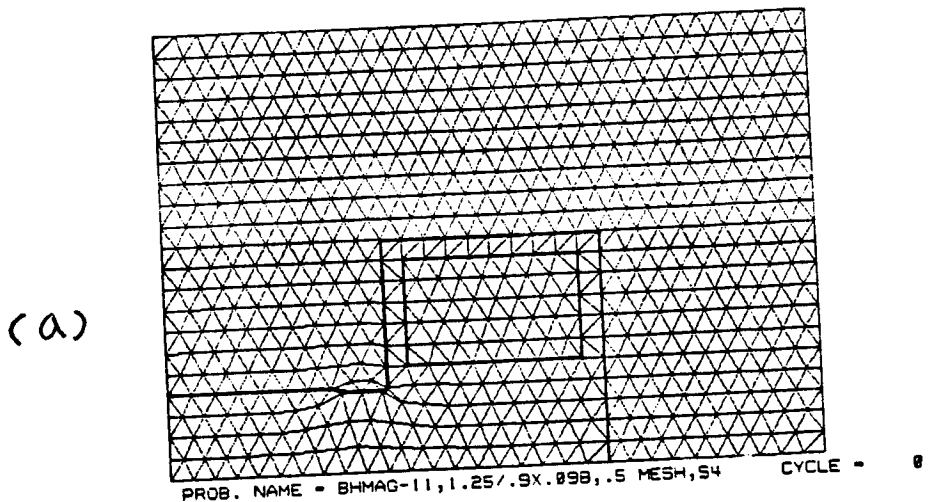


Fig. 2. (a) 0.5 cm x 0.5 cm equal weight triangle meshes and (b) flux lines of a POISSON run. The shim is not a separate iron region in this run.

- #1 POISSON run with  $0.25 \times 0.25 \text{ cm}^2$  mesh
- #2 POISSON run with  $0.125 \times 0.125 \text{ cm}^2$  mesh
- #3 LINDA run with  $0.25 \times 0.25 \text{ cm}^2$  mesh
- #4 LINDA run with  $0.125 \times 0.125 \text{ cm}^2$  mesh
- #5 LINDA run with  $0.5 \times 0.5 \text{ cm}^2$  mesh
- #6 LINDA run with  $0.125 \times 0.25 \text{ cm}^2$  mesh
- #7 LINDA run with  $0.125 \times 0.0625 \text{ cm}^2$  mesh
- #8 LINDA run with  $0.5 \times 0.25 \text{ cm}^2$  mesh
- #9 LINDA run with  $0.25 \times 0.5 \text{ cm}^2$  mesh

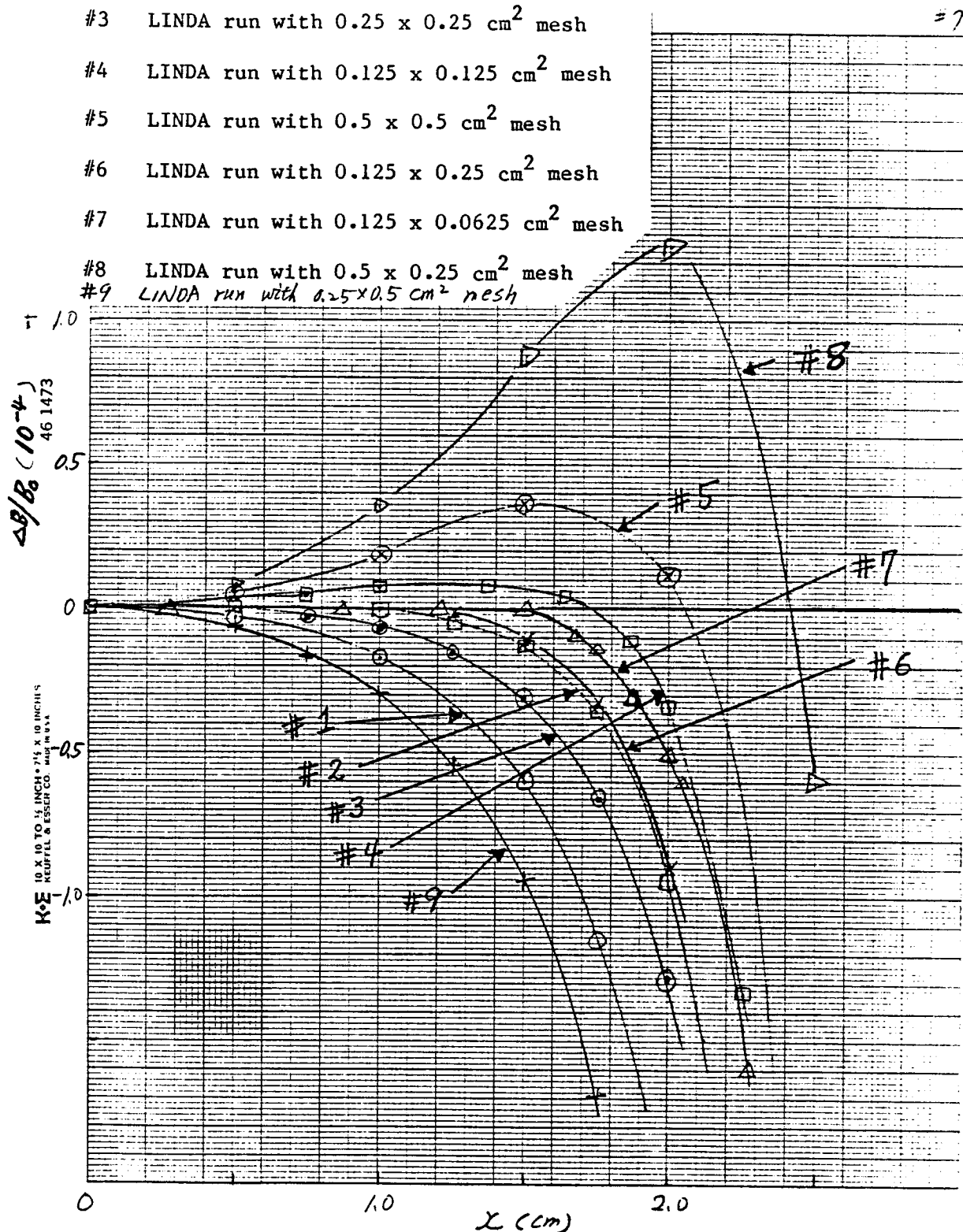


Fig. 3. Variations of  $\Delta B/B_0$  along  $y = 0$  symmetry plane of POISSON and LINDA runs. All POISSON runs used equal weight triangle meshes and LINDA rectangle meshes. The shim thickness is 0.92 mm and Fermilab B-H Table is used.

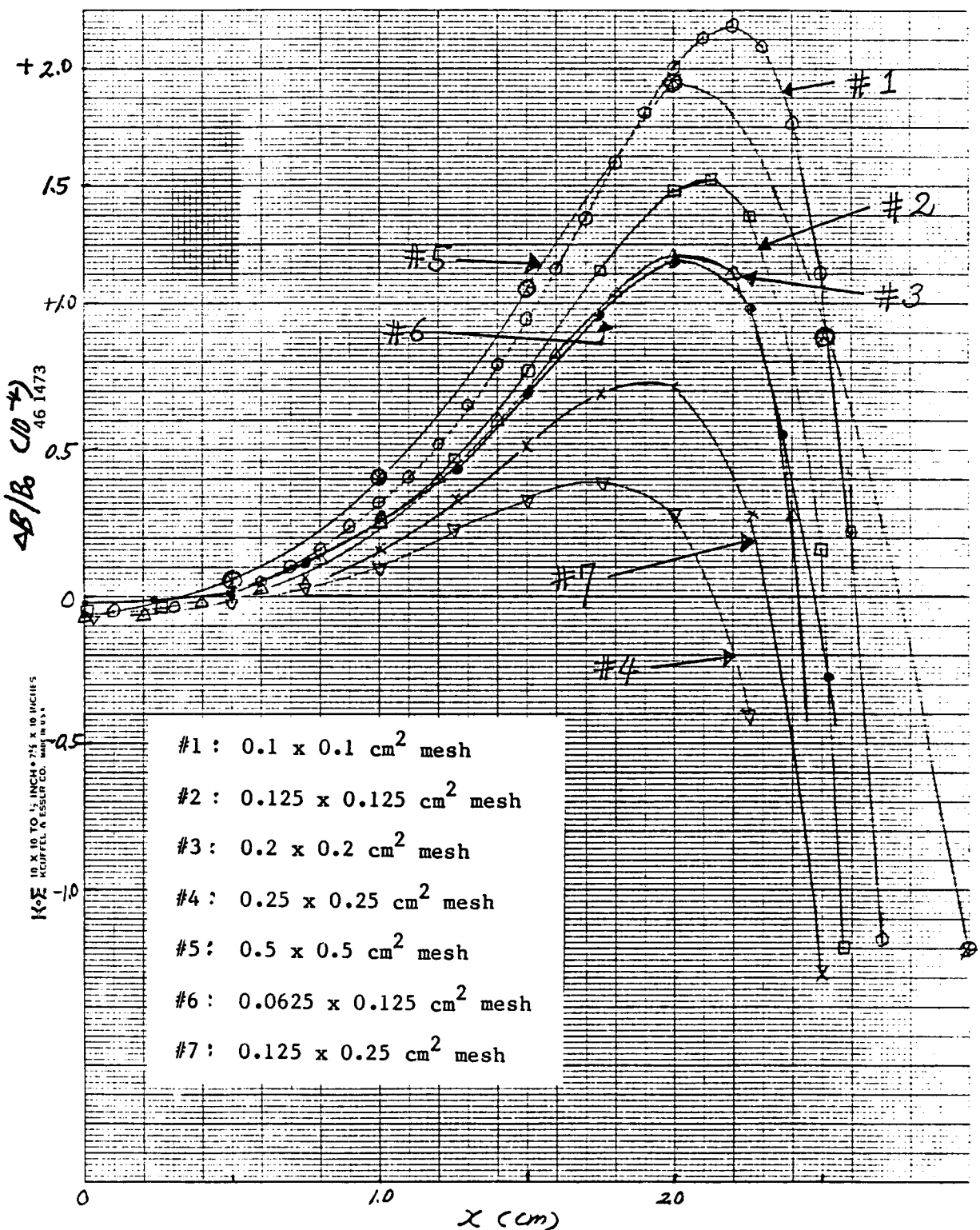


Fig. 4. LINDA runs using Fermilab B-H Table with shim thickness of 0.98 mm.

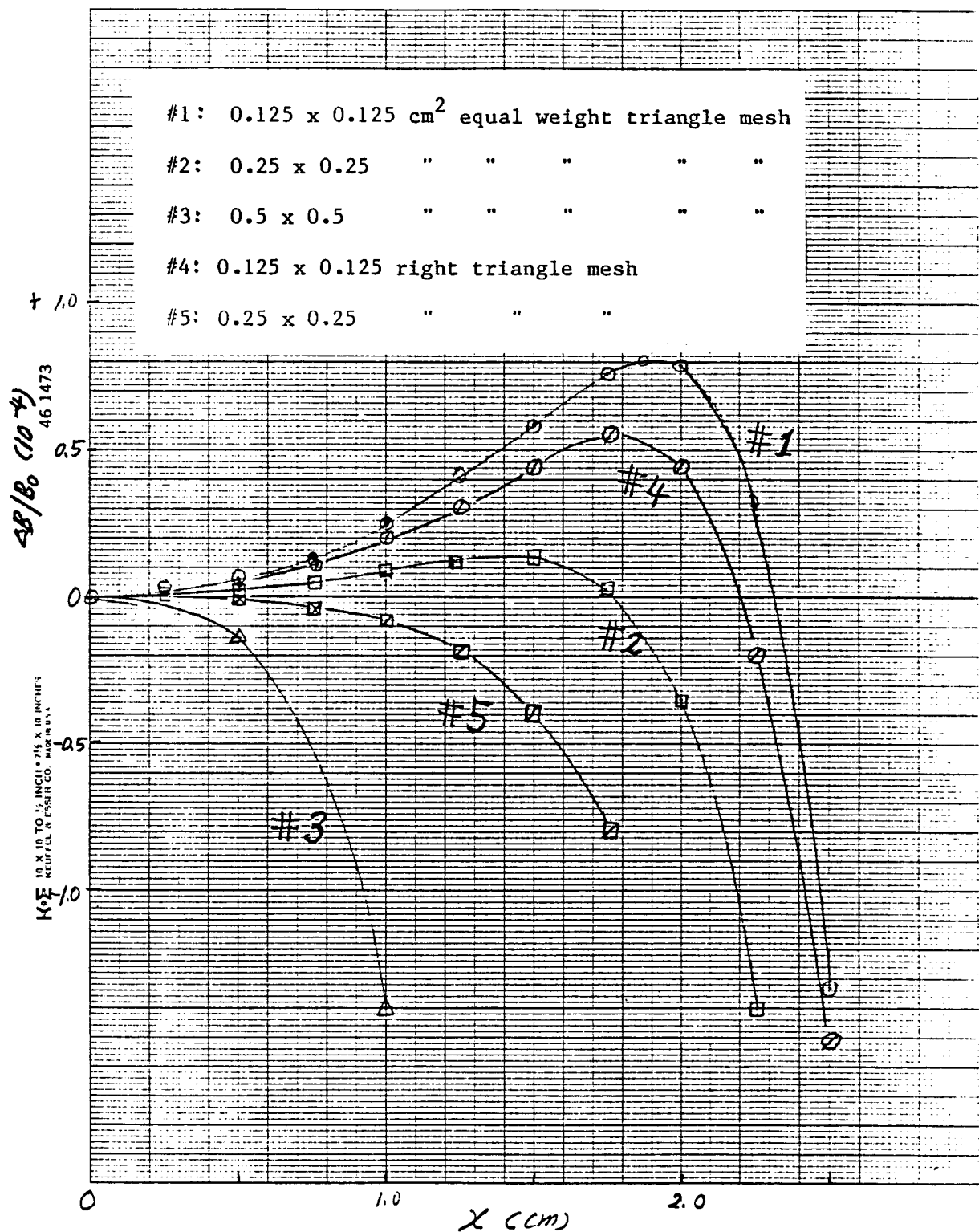


Fig. 5. POISSON runs of two different kinds of meshes with shim thickness of 0.98 mm. Fermilab B-H Table is used.

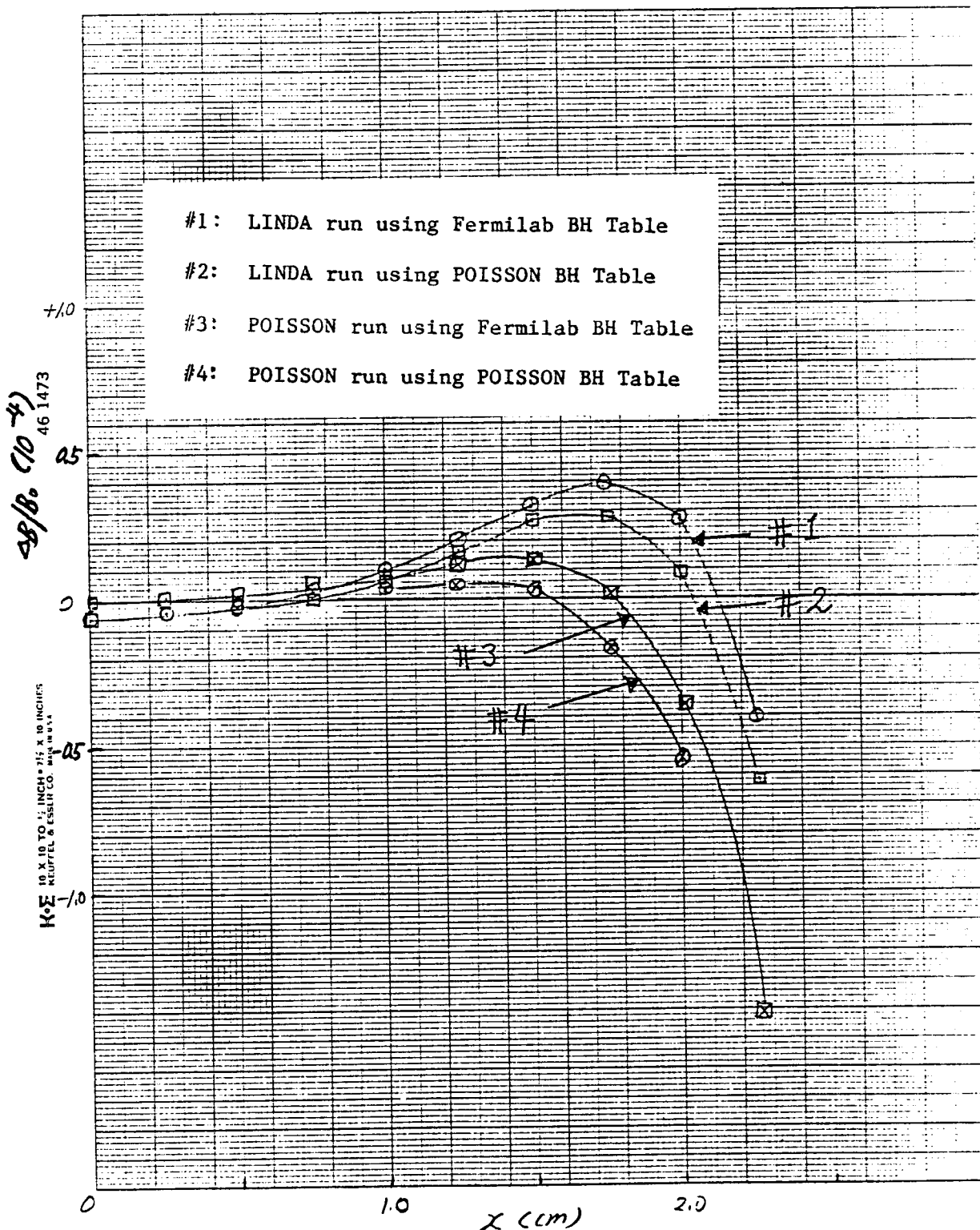


Fig. 6. LINDA and POISSON runs of 0.25 cm x 0.25 cm meshes using two different B-H Tables. Shim thickness is 0.98 mm.

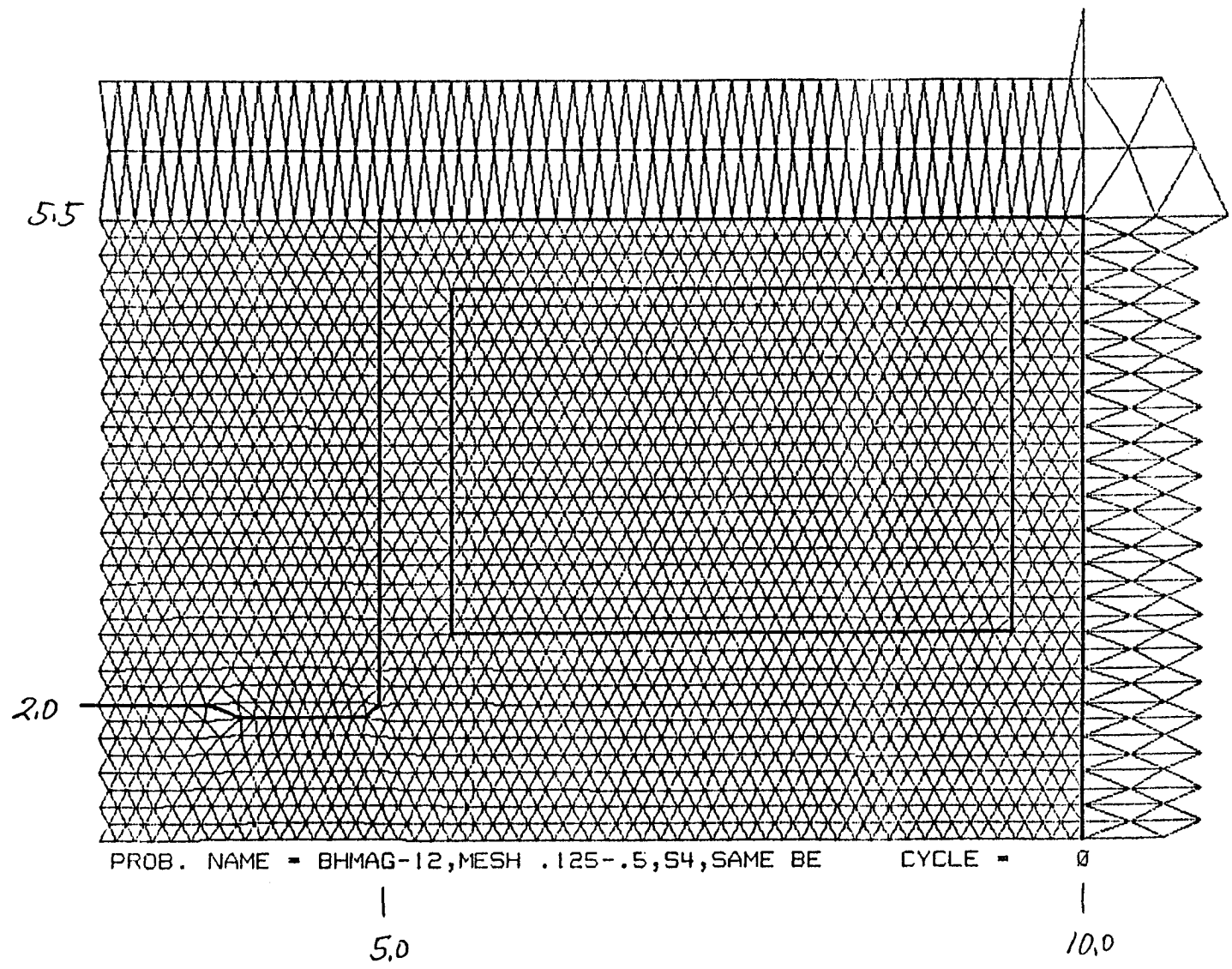
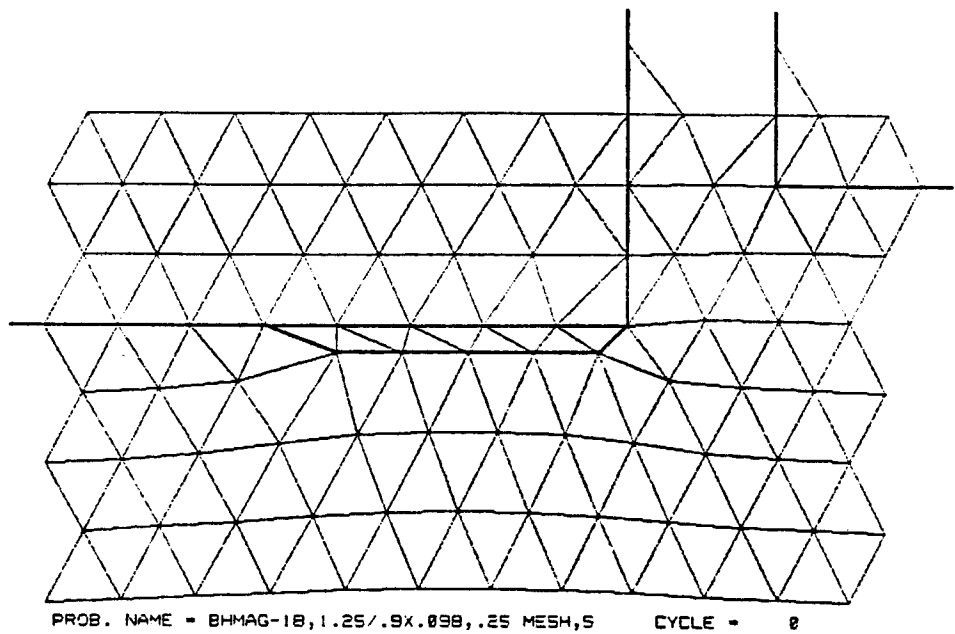


Fig. 7. Non-uniform triangle meshes near the coil region are shown for a POISSON run. Horizontal mesh intervals are 0.125 cm and 0.5 cm for  $0 < x < 10.0$  and  $10.0 < x < 15.0$ , respectively. Vertical intervals are also 0.125 cm and 0.5 cm for  $0 < y < 5.5$  and  $5.5 < y < 10.5$ . The shim thickness is 0.98 mm.

(a)



(b)

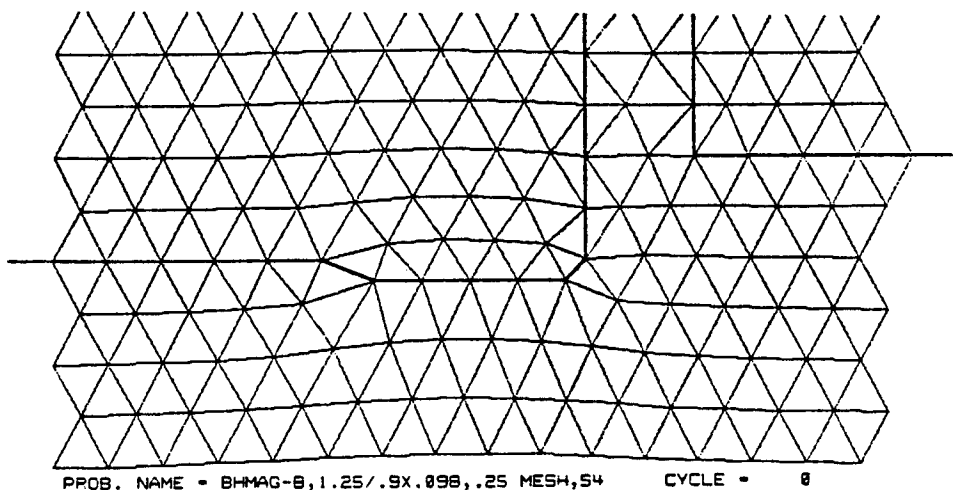


Fig. 8. Mesh distortion near 0.98 mm-thick shim. Far away from the shim, 0.25 cm x 0.25 cm uniform meshes are used. (a) Shim as a separate iron region, (b) Shim as a part of the whole iron region.

# M TYPES IBM 360

- 1 NOFLUX IBODYF=1 XA(3),YA(3)  
 IRON  
 NOFLUX IBODXF=1 XA(1),YA(1)  
 FLUX NORMAL IBODYO=0 XA(2),YA(2)
- C Magnet!  
 Quadrant 2  
 (Define special points XA,YA)
- 2 Assymmetric H Magnet  
 Quadrants 1 and 2
- 3 Quadrupole Magnet.  
 Quadrant 1
- 4 Sextupole or  $\frac{1}{2}$  Symmetrical H Magnet, Quadrant 2
- 5 Collins Quadrupole  
 Quadrant 1
- 6 C Magnet with no Inaccessible Air, Quadrant 2

Fig. 9. Magnet types allowed in the present version of LINDA.

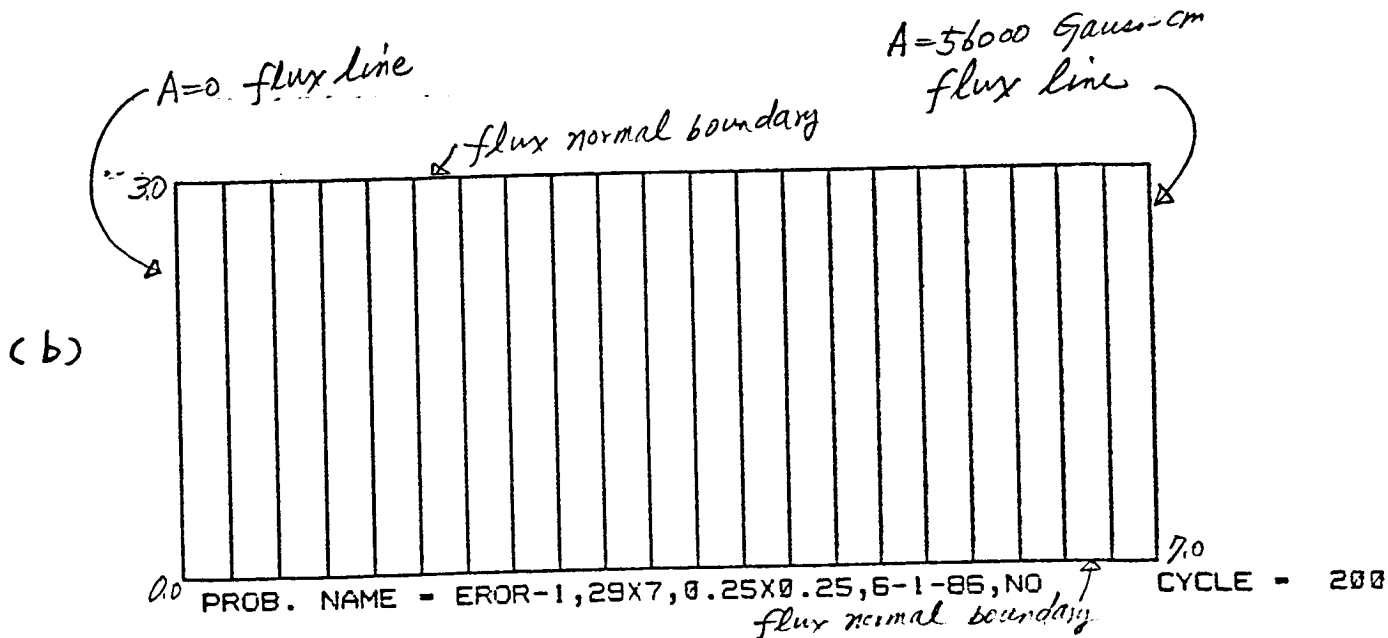
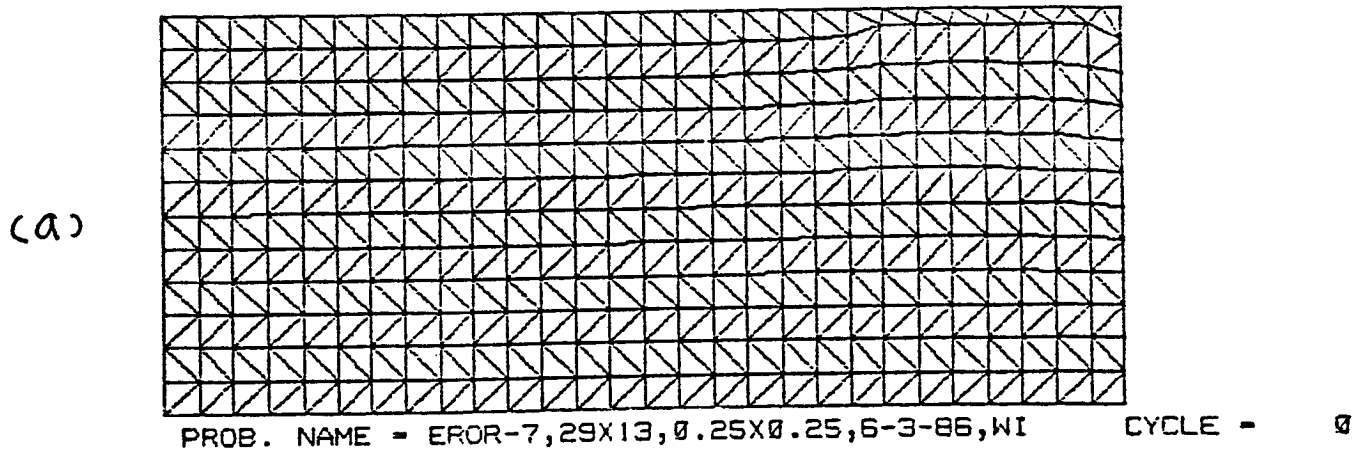


Fig. 10. Perfect dipole using  $0.25 \text{ cm} \times 0.25 \text{ cm}$  right angle triangle meshes. (a) Mesh distortion near the shim, (b) Flux lines with vector potentials of  $A = 0$  at  $x = 0$ , and  $A = 56000 \text{ Gauss-cm}$  at  $x = 7.0$ .

Table 1 - Fermilab B-H table

N	B-SQUARED	B(GAUSS)	GAMMA	MU	H(OERSTEAD)	D-GAM/D-BSQ
1	0.000000E+00	0.00	0.000100	10000.00	0.00	3.8000E-09
2	1.000000E+08	10000.00	0.000138	7246.38	1.38	-2.9093E-14
3	1.210000E+08	11000.00	0.000141	7096.78	1.55	-7.5140E-14
4	1.440000E+08	12000.00	0.000150	6666.67	1.80	-1.3356E-13
5	1.690000E+08	13000.00	0.000169	5909.09	2.20	-3.0889E-13
6	1.960000E+08	14000.00	0.000221	4516.13	3.10	-9.7918E-13
7	2.250000E+08	15000.00	0.000413	2419.35	6.20	-1.6039E-12
8	2.402500E+08	15500.00	0.000774	1291.67	12.00	-2.5009E-12
9	2.560000E+08	16000.00	0.001375	727.27	22.00	-3.3886E-12
10	2.722500E+08	16500.00	0.002242	445.95	37.00	-3.6471E-12
11	2.890000E+08	17000.00	0.003235	309.09	55.00	-4.2281E-12
12	3.062500E+08	17500.00	0.004457	224.36	78.00	-4.4939E-12
13	3.240000E+08	18000.00	0.005833	171.43	105.00	-4.0181E-12
14	3.422500E+08	18500.00	0.007135	140.15	132.00	-4.0650E-12
15	3.610000E+08	19000.00	0.008526	117.28	162.00	-3.6563E-12
16	3.802500E+08	19500.00	0.009846	101.56	192.00	-3.5606E-12
17	4.000000E+08	20000.00	0.011200	89.29	224.00	-3.3416E-12
18	4.202500E+08	20500.00	0.012537	79.77	257.00	-3.2558E-12
19	4.410000E+08	21000.00	0.013905	71.92	292.00	-6.4389E-12
20	4.622500E+08	21500.00	0.016744	59.72	360.00	-2.0319E-11
21	4.840000E+08	22000.00	0.026136	38.26	575.00	-3.7828E-11
22	5.062500E+08	22500.00	0.044444	22.50	1000.00	-3.8458E-11
23	5.290000E+08	23000.00	0.063913	15.65	1470.00	-7.2947E-11
24	5.760000E+08	24000.00	0.102500	9.76	2460.00	-5.8162E-11
25	6.250000E+08	25000.00	0.136000	7.35	3400.00	-2.3041E-10
26	9.000000E+08	30000.00	0.280000	3.57	8400.00	-1.9723E-10
27	1.600000E+09	40000.00	0.457500	2.19	18300.00	-2.2554E-10
28	1.440000E+10	120000.01	0.818333	1.22	98200.01	

RECONSTRUCTION OF THE TABLE FOR MAT. NO. 4 WITH EQUAL INCREMENTS OF B-SQUARED

MAXIMUM B-SQUARED = 2.799997E+09, WITH TRUNCATION FOR HIGHER VALUES

B-SQUARED INCREMENT = 6.999993E+06

Table 2 - POISSON B-H Table

N	B-SQUARED	B(GAUSS)	GAMMA	MU	H(DERSTEAD)	D-GAM/D-BSQ
1	0. 000000E+00	0. 00	0. 000250	4000. 00	0. 00	0. 0000E+00
2	7. 999996E+07	8944. 27	0. 000250	4000. 00	2. 24	-7. 2511E-13
3	1. 440000E+08	12000. 00	0. 000308	3246. 75	3. 70	-9. 8621E-13
4	1. 960000E+08	14000. 00	0. 000450	2222. 22	6. 30	-1. 1072E-12
5	2. 250000E+08	15000. 00	0. 000667	1499. 25	10. 01	-1. 1912E-12
6	2. 402500E+08	15500. 00	0. 000935	1069. 52	14. 49	-1. 9772E-12
7	2. 560000E+08	16000. 00	0. 001410	709. 22	22. 56	-3. 0080E-12
8	2. 722500E+08	16500. 00	0. 002180	458. 72	35. 97	-3. 8937E-12
9	2. 890000E+08	17000. 00	0. 003240	308. 64	55. 08	-3. 8065E-12
10	3. 062500E+08	17500. 00	0. 004340	230. 41	75. 95	-4. 3431E-12
11	3. 240000E+08	18000. 00	0. 005670	176. 37	102. 06	-4. 6916E-12
12	3. 422500E+08	18500. 00	0. 007190	139. 08	133. 01	-5. 2888E-12
13	3. 610000E+08	19000. 00	0. 009000	111. 11	171. 00	-5. 8175E-12
14	3. 802500E+08	19500. 00	0. 011100	90. 09	216. 45	-5. 7860E-12
15	4. 000000E+08	20000. 00	0. 013300	75. 19	266. 00	-7. 7504E-12
16	4. 202500E+08	20500. 00	0. 016400	60. 98	336. 20	-9. 0427E-12
17	4. 410000E+08	21000. 00	0. 020200	49. 50	424. 20	-5. 4424E-12
18	4. 515583E+08	21249. 90	0. 022600	44. 25	480. 25	-6. 6440E-12
19	4. 622500E+08	21500. 00	0. 025600	39. 06	550. 40	-1. 0168E-11
20	4. 730625E+08	21750. 00	0. 030300	33. 00	659. 03	-1. 5643E-11
21	4. 840000E+08	22000. 00	0. 037700	26. 53	829. 40	-3. 6892E-11
22	5. 062500E+08	22500. 00	0. 055555	18. 00	1249. 99	-2. 1951E-11
23	5. 196850E+08	22796. 60	0. 066667	15. 00	1519. 78	-1. 9736E-11
24	5. 321603E+08	23068. 60	0. 076923	13. 00	1774. 51	-2. 6283E-11
25	5. 495743E+08	23443. 00	0. 090909	11. 00	2131. 18	-3. 6761E-11
26	5. 757888E+08	23995. 60	0. 111111	9. 00	2666. 18	-5. 5137E-11
27	6. 202590E+08	24905. 00	0. 142857	7. 00	3557. 85	-3. 8389E-11
28	6. 567533E+08	25627. 20	0. 166667	6. 00	4271. 21	-5. 0756E-11
29	7. 132104E+08	26706. 00	0. 200000	5. 00	5341. 20	-7. 0108E-11
30	8. 121417E+08	28498. 10	0. 250000	4. 00	7124. 52	-1. 0261E-10
31	1. 028722E+09	32073. 70	0. 333330	3. 00	10691. 13	-6. 4811E-11
32	1. 270502E+09	35644. 10	0. 400000	2. 50	14257. 64	-7. 8712E-11
33	1. 830334E+09	42782. 40	0. 500000	2. 00	21391. 20	-3. 0350E-11
34	2. 316901E+09	48134. 20	0. 555550	1. 80	26740. 95	-2. 9976E-11
35	3. 254896E+09	57051. 70	0. 625000	1. 60	35657. 31	-1. 2802E-11
36	4. 119804E+09	64185. 70	0. 666667	1. 50	42790. 49	-1. 1559E-11
37	5. 608093E+09	74887. 20	0. 714285	1. 40	53490. 81	

RECONSTRUCTION OF THE TABLE FOR MAT. NO. 2 WITH EQUAL INCREMENTS OF B-SQUARED

MAXIMUM B-SQUARED = 2. 799997E+09, WITH TRUNCATION FOR HIGHER VALUES

B-SQUARED INCREMENT = 6. 999993E+06

Table 3 - Magnetic field and vector potential of Fig. 5, #1  
 (0.125 cm x 0.125 cm uniform meshes).

K	L	A(VECTOR)	X(CM)	Y(CM)	BX(GAUSS)	BY(GAUSS)
1	1	0.000000E+00	0.00000	0.00000	0.000	6986.826
2	1	-8.733534E+02	0.12500	0.00000	0.000	6986.828
3	1	-1.746707E+03	0.25000	0.00000	0.000	6986.835
4	1	-2.620063E+03	0.37500	0.00000	0.000	6986.848
5	1	-3.493420E+03	0.50000	0.00000	0.000	6986.867
6	1	-4.366779E+03	0.62500	0.00000	0.000	6986.886
7	1	-5.240142E+03	0.75000	0.00000	0.000	6986.920
8	1	-6.113509E+03	0.87500	0.00000	0.000	6986.958
9	1	-6.986881E+03	1.00000	0.00000	0.000	6987.000
10	1	-7.860259E+03	1.12500	0.00000	0.000	6987.048
11	1	-8.733645E+03	1.25000	0.00000	0.000	6987.103
12	1	-9.607037E+03	1.37500	0.00000	0.000	6987.169
13	1	-1.048044E+04	1.50000	0.00000	0.000	6987.237
14	1	-1.135385E+04	1.62500	0.00000	0.000	6987.310
15	1	-1.222726E+04	1.75000	0.00000	0.000	6987.359
16	1	-1.310069E+04	1.87500	0.00000	0.000	6987.394
17	1	-1.397411E+04	2.00000	0.00000	0.000	6987.381
18	1	-1.484753E+04	2.12500	0.00000	0.000	6987.285
19	1	-1.572093E+04	2.25000	0.00000	0.000	6987.059
20	1	-1.659429E+04	2.37500	0.00000	0.000	6986.628
21	1	-1.746757E+04	2.50000	0.00000	0.000	6985.890
22	1	-1.834074E+04	2.62500	0.00000	0.000	6984.669
23	1	-1.921371E+04	2.75000	0.00000	0.000	6982.774
24	1	-2.008639E+04	2.87500	0.00000	0.000	6979.882
25	1	-2.095862E+04	3.00000	0.00000	0.000	6975.631

Table 4 - Magnetic field and vector potential using non-uniform meshes of Fig. 7 (0.125 cm ~ 0.5 cm meshes).

K	L	A(VECTOR)	X(cm)	Y(cm)	BX(GAUSS)	BY(GAUSS)
1	1	0.000000E+00	0.00000	0.00000	0.000	6986.677
2	1	-8.733348E+02	0.12500	0.00000	0.000	6986.680
3	1	-1.746670E+03	0.25000	0.00000	0.000	6986.686
4	1	-2.620007E+03	0.37500	0.00000	0.000	6986.699
5	1	-3.493345E+03	0.50000	0.00000	0.000	6986.717
6	1	-4.366687E+03	0.62500	0.00000	0.000	6986.738
7	1	-5.240031E+03	0.75000	0.00000	0.000	6986.771
8	1	-6.113379E+03	0.87500	0.00000	0.000	6986.805
9	1	-6.986732E+03	1.00000	0.00000	0.000	6986.851
10	1	-7.860092E+03	1.12500	0.00000	0.000	6986.901
11	1	-8.733458E+03	1.25000	0.00000	0.000	6986.955
12	1	-9.606832E+03	1.37500	0.00000	0.000	6987.024
13	1	-1.048021E+04	1.50000	0.00000	0.000	6987.089
14	1	-1.135360E+04	1.62500	0.00000	0.000	6987.153
15	1	-1.222700E+04	1.75000	0.00000	0.300	6987.211
16	1	-1.310041E+04	1.87500	0.00000	0.000	6987.239
17	1	-1.397381E+04	2.00000	0.00000	0.000	6987.230
18	1	-1.484721E+04	2.12500	0.00000	0.000	6987.133
19	1	-1.572059E+04	2.25000	0.00000	0.000	6986.910
20	1	-1.659393E+04	2.37500	0.00000	0.000	6986.479
21	1	-1.746720E+04	2.50000	0.00000	0.300	6985.737
22	1	-1.834034E+04	2.62500	0.00000	0.000	6984.510
23	1	-1.921330E+04	2.75000	0.00000	0.300	6982.622
24	1	-2.008596E+04	2.87500	0.00000	0.000	6979.729
25	1	-2.095817E+04	3.00000	0.00000	0.000	6975.463

Table 5 - Comparison of harmonic analysis. (a): uniform meshes of Table 3  
and (b): non-uniform meshes of Table 4.

TABLE FOR FIELD COEFFICIENTS

NORMALIZATION RADIUS = 1.75000

(a)

$$(3X - I \cdot 3Y) = I * \text{SUM } N * (A_N + I \cdot B_N) / R * (Z/R)^{N-1}$$

N	N(A <sub>N</sub> )/R	N(B <sub>N</sub> )/R	ABS(N(C <sub>N</sub> )/R)	b <sub>n</sub>	a <sub>n</sub> = 0
1	-6.9863E+03	0.0000E+00	6.9863E+03	b <sub>0</sub> = 1.0	
3	-4.6070E-01	0.0000E+00	4.6070E-01	b <sub>1</sub> = 0	b <sub>2</sub> = 2.15E+0 <sup>-5</sup>
5	-2.3291E-01	0.0000E+00	2.3291E-01	b <sub>4</sub> = 3.55E+0 <sup>-6</sup>	
7	5.6176E-02	0.0000E+00	5.6176E-02	b <sub>6</sub> = -2.77E+0 <sup>-7</sup>	
9	6.8638E-02	0.0000E+00	6.8638E-02	b <sub>8</sub> = -1.11E+0 <sup>-7</sup>	
11	1.4615E-02	0.0000E+00	1.4615E-02	b <sub>10</sub> = -7.75E+0 <sup>-9</sup>	
13	2.7636E-03	0.0000E+00	2.7636E-03	b <sub>12</sub> = -4.99E+0 <sup>-10</sup>	
15	9.1677E-03	0.0000E+00	9.1677E-03	b <sub>14</sub> = -5.18E+0 <sup>-10</sup>	
17	-3.1622E-03	0.0000E+00	3.1622E-03	b <sub>16</sub> = 5.84E+0 <sup>-11</sup>	
19	-1.5652E-02	0.0000E+00	1.5652E-02	b <sub>18</sub> = 9.43E+0 <sup>-11</sup>	

(b)

TABLE FOR FIELD COEFFICIENTS

NORMALIZATION RADIUS = 1.75000

$$(3X - I \cdot 3Y) = I * \text{SUM } N * (A_N + I \cdot B_N) / R * (Z/R)^{N-1}$$

N	N(A <sub>N</sub> )/R	N(B <sub>N</sub> )/R	ABS(N(C <sub>N</sub> )/R)	b <sub>n</sub>	a <sub>n</sub> = 0
1	-6.9867E+03	0.0000E+00	6.9867E+03		
3	-4.6078E-01	0.0000E+00	4.6078E-01		
5	-2.3424E-01	0.0000E+00	2.3424E-01		
7	5.8966E-02	0.0000E+00	5.8966E-02		
9	7.2465E-02	0.0000E+00	7.2465E-02		
11	1.8707E-02	0.0000E+00	1.8707E-02		
13	7.9454E-03	0.0000E+00	7.9454E-03		
15	5.9790E-03	0.0000E+00	5.9790E-03		
17	-4.9692E-03	0.0000E+00	4.9692E-03		

Table 6 - Magnetic field and vector potential from Fig. 8(b) meshes  
 (curve Fig. 6, #4).

K	L	A(VECTOR)	X(cm)	Y(cm)	BX(GAUSS)	BY(GAUSS)
1	1	0. 000000E+00	0. 00000	0. 00000	0. 000	6973. 496
2	1	-1. 743374E+03	0. 25000	0. 00000	0. 000	6973. 499
3	1	-3. 486749E+03	0. 50000	0. 00000	0. 000	6973. 502
4	1	-5. 230126E+03	0. 75000	0. 00000	0. 000	6973. 514
5	1	-6. 973506E+03	1. 00000	0. 00000	0. 000	6973. 525
6	1	-8. 716889E+03	1. 25000	0. 00000	0. 000	6973. 531
7	1	-1. 046027E+04	1. 50000	0. 00000	0. 000	6973. 516
8	1	-1. 220364E+04	1. 75000	0. 00000	0. 000	6973. 415
9	1	-1. 394696E+04	2. 00000	0. 00000	0. 000	6973. 115
10	1	-1. 569016E+04	2. 25000	0. 00000	0. 000	6972. 333
11	1	-1. 743304E+04	2. 50000	0. 00000	0. 000	6970. 496
12	1	-1. 917522E+04	2. 75000	0. 00000	0. 000	6966. 451
13	1	-2. 091590E+04	3. 00000	0. 00000	0. 000	6958. 039
14	1	-2. 265356E+04	3. 25000	0. 00000	0. 000	6941. 483
15	1	-2. 438545E+04	3. 50000	0. 00000	0. 000	6910. 734
16	1	-2. 610700E+04	3. 75000	0. 00000	0. 000	6856. 989
17	1	-2. 781108E+04	4. 00000	0. 00000	0. 000	6768. 908
18	1	-2. 948757E+04	4. 25000	0. 00000	0. 000	6634. 044
19	1	-3. 112334E+04	4. 50000	0. 00000	0. 000	6441. 598
20	1	-3. 270315E+04	4. 75000	0. 00000	0. 000	6186. 043
21	1	-3. 421134E+04	5. 00000	0. 00000	0. 000	5869. 862
22	1	-3. 563394E+04	5. 25000	0. 00000	0. 000	5503. 918
23	1	-3. 696051E+04	5. 50000	0. 00000	0. 000	5104. 698
24	1	-3. 818499E+04	5. 75000	0. 00000	0. 000	4690. 149
25	1	-3. 930560E+04	6. 00000	0. 00000	0. 000	4276. 032

Table 7 - Magnetic field and vector potential from Fig. 8(a) meshes.

	$x$	$y$	$A(\text{VOLTM})$	$\lambda (\text{cm})$	$T(\text{cm})$	$\Delta A(\text{Gauss})$	$\Delta Y(\text{GAUSS})$
1	1	1	0.000000E+00	0.000000	0.000000	0.000	6973.494
2	1	2	-1.743374E+03	0.250000	0.000000	0.000	6973.496
3	1	3	-3.486749E+03	0.500000	0.000000	0.000	6973.500
4	1	4	-5.230125E+03	0.750000	0.000000	0.000	6973.511
5	1	5	-6.973504E+03	1.000000	0.000000	0.000	6973.524
6	1	6	-8.716887E+03	1.250000	0.000000	0.000	6973.530
7	1	7	-1.045927E+04	1.500000	0.000000	0.000	6973.514
8	1	8	-1.220394E+04	1.750000	0.000000	0.000	6973.411
9	1	9	-1.394695E+04	2.000000	0.000000	0.000	6973.113
10	1	10	-1.569015E+04	2.250000	0.000000	0.000	6972.333
11	1	11	-1.743304E+04	2.500000	0.000000	0.000	6970.494
12	1	12	-1.917521E+04	2.750000	0.000000	0.000	6906.452
13	1	13	-2.091589E+04	3.000000	0.000000	0.000	6958.036
14	1	14	-2.265355E+04	3.250000	0.000000	0.000	6941.406
15	1	15	-2.438545E+04	3.500000	0.000000	0.000	6910.733
16	1	16	-2.610099E+04	3.750000	0.000000	0.000	6850.992
17	1	17	-2.781133E+04	4.000000	0.000000	0.000	6768.910
18	1	18	-2.948755E+04	4.250000	0.000000	0.000	6634.045
19	1	19	-3.112334E+04	4.500000	0.000000	0.000	6441.595
20	1	20	-3.270315E+04	4.750000	0.000000	0.000	6186.044
21	1	21	-3.421133E+04	5.000000	0.000000	0.000	5869.862
22	1	22	-3.563374E+04	5.250000	0.000000	0.000	5503.924
23	1	23	-3.695050E+04	5.500000	0.000000	0.000	5104.695
24	1	24	-3.813495E+04	5.750000	0.000000	0.000	4690.146
25	1	25	-3.930559E+04	6.000000	0.000000	0.000	4270.024

Table 8 - Comparison of harmonic analysis. (a): Fig. 8(b) meshes,  
and (b): Fig. 8(a) meshes.

TABLE FOR FIELD COEFFICIENTS

NORMALIZATION RADIUS = 1.75000

$$(BX - I BY) = I * \text{SUM } N * (AN + I BN) / R * (Z/R)^{**(N-1)}$$

(a)	N	N(AN)/R	N(BN)/R	ABS(N(CN)/R)
	1	-6.9735E+03	0.0000E+00	6.9735E+03
	3	-9.5576E-02	0.0000E+00	9.5576E-02
	5	-3.2721E-02	0.0000E+00	3.2721E-02
	7	1.1186E-01	0.0000E+00	1.1186E-01
	9	8.6293E-02	0.0000E+00	8.6293E-02
	11	2.9576E-02	0.0000E+00	2.9576E-02
	13	8.5735E-03	0.0000E+00	8.5735E-03
	15	3.8048E-03	0.0000E+00	3.8048E-03
	17	6.0369E-03	0.0000E+00	6.0369E-03

, (b) SHIM : SEPARATE REGION

925	1	TABLE FOR FIELD COEFFICIENTS		
926	0	NORMALIZATION RADIUS = 1.75000		
927	0	$(BX - I BY) = I * \text{SUM } N * (AN + I BN) / R * (Z/R)^{**(N-1)}$		
928	0	N	N(AN)/R	N(BN)/R
929	0	1	-6.9735E+03	0.0000E+00
930	0	3	-9.6642E-02	0.0000E+00
931	0	5	-3.4243E-02	0.0000E+00
932	0	7	1.1506E-01	0.0000E+00
933	0	9	8.8119E-02	0.0000E+00
934	0	11	2.8460E-02	0.0000E+00
935	0	13	5.2760E-03	0.0000E+00
936	0	15	5.3267E-03	0.0000E+00
937	0	17	8.6242E-03	0.0000E+00

Table 9 - Magnetic field and vector potential of a perfect dipole field with uniform 0.25 cm x 0.25 cm right angle triangle meshes.

<i>K</i>	<i>L</i>	<i>A(VECTOR)</i>	<i>X(cm)</i>	<i>y(cm)</i>	<i>B<sub>x</sub>(Gauss)</i>	<i>B<sub>y</sub>(Gauss)</i>
26	1	5.000000E+04	6.25000	0.00000	0.000	-7999.986
27	1	5.200000E+04	6.50000	0.00000	0.000	-8000.002
28	1	5.400000E+04	6.75000	0.00000	0.000	-7999.996
29	1	5.600000E+04	7.00000	0.00000	0.000	-8000.017
1	2	0.000000E+00	0.00000	0.25000	0.000	-7999.973
2	2	1.999992E+03	0.25000	0.25000	0.002	-7999.974
3	2	3.999987E+03	0.50000	0.25000	0.000	-7999.966
4	2	5.999980E+03	0.75000	0.25000	-0.004	-7999.972
5	2	7.999974E+03	1.00000	0.25000	-0.010	-7999.979
6	2	9.999969E+03	1.25000	0.25000	-0.003	-7999.981
7	2	1.199996E+04	1.50000	0.25000	0.004	-7999.996
8	2	1.399997E+04	1.75000	0.25000	-0.006	-8000.004
9	2	1.599998E+04	2.00000	0.25000	-0.010	-8000.003
10	2	1.799997E+04	2.25000	0.25000	-0.007	-7999.978
11	2	1.999997E+04	2.50000	0.25000	0.004	-8000.005
12	2	2.199998E+04	2.75000	0.25000	0.000	-8000.018
13	2	2.399998E+04	3.00000	0.25000	-0.002	-8000.025
14	2	2.599999E+04	3.25000	0.25000	-0.011	-8000.004
15	2	2.799998E+04	3.50000	0.25000	-0.014	-7999.993
16	2	2.999998E+04	3.75000	0.25000	-0.001	-7999.995
17	2	3.199998E+04	4.00000	0.25000	0.009	-8000.004
18	2	3.399998E+04	4.25000	0.25000	0.003	-8000.019
19	2	3.600000E+04	4.50000	0.25000	0.020	-8000.019
20	2	3.800001E+04	4.75000	0.25000	0.016	-8000.032
21	2	4.000002E+04	5.00000	0.25000	0.006	-8000.019
22	2	4.200001E+04	5.25000	0.25000	0.005	-8000.011
23	2	4.400002E+04	5.50000	0.25000	-0.006	-8000.004
24	2	4.600002E+04	5.75000	0.25000	0.011	-8000.000
25	2	4.800002E+04	6.00000	0.25000	0.004	-7999.998
26	2	5.000000E+04	6.25000	0.25000	-0.006	-8000.002

Table 10 - Magnetic field and vector potential of a perfect dipole field with distorted meshes of Fig. 10(a).

	<i>K</i>	<i>L</i>	<i>A</i> (VECTOR)	<i>X</i> (cm)	<i>Y</i> (cm)	<i>B<sub>x</sub></i> (Gauss)	<i>B<sub>y</sub></i> (Gauss)
	26	1	5.000001E+04	6.25000	0.00000	0.000	-7999.982
	27	1	5.200001E+04	6.50000	0.00000	0.003	-7999.984
	28	1	5.400000E+04	6.75000	0.00000	0.000	-7999.980
	29	1	5.600000E+04	7.00000	0.00000	0.000	-8000.011
	1	2	0.000000E+00	0.00000	0.25000	0.000	-8000.023
	2	2	2.000007E+03	0.25000	0.25001	-0.003	-8000.019
	3	2	4.000015E+03	0.50000	0.25003	-0.008	-8000.031
	4	2	6.000024E+03	0.75000	0.25006	-0.013	-8000.025
	5	2	8.000022E+03	1.00000	0.25011	-0.006	-8000.011
	6	2	1.000003E+04	1.25000	0.25012	0.004	-8000.020
	7	2	1.200004E+04	1.50000	0.25020	0.003	-8000.030
	8	2	1.400004E+04	1.75000	0.25026	-0.002	-8000.023
	9	2	1.600005E+04	2.00000	0.25034	-0.015	-8000.012
	10	2	1.800004E+04	2.25000	0.25044	-0.021	-7999.999
	11	2	2.000004E+04	2.50000	0.25055	-0.021	-7999.984
	12	2	2.200004E+04	2.75000	0.25071	-0.021	-7999.976
	13	2	2.400003E+04	3.00000	0.25089	-0.018	-7999.975
	14	2	2.600002E+04	3.25000	0.25111	-0.014	-7999.987
	15	2	2.800002E+04	3.50000	0.25137	-0.009	-7999.988
	16	2	3.000003E+04	3.75000	0.25168	-0.012	-8000.001
	17	2	3.200003E+04	4.00000	0.25202	-0.013	-8000.008
	18	2	3.400004E+04	4.25000	0.25238	-0.019	-8000.000
	19	2	3.600003E+04	4.50000	0.25276	-0.019	-7999.990
	20	2	3.800004E+04	4.75000	0.25311	-0.009	-8000.002
	21	2	4.000003E+04	5.00000	0.25339	-0.017	-8000.000
	22	2	4.200002E+04	5.25000	0.25358	-0.004	-7999.992
	23	2	4.400002E+04	5.50000	0.25351	-0.015	-7999.996
	24	2	4.600003E+04	5.75000	0.25346	-0.009	-7999.990
	25	2	4.800002E+04	6.00000	0.25311	-0.008	-7999.987
	26	2	5.000002E+04	6.25000	0.25255	-0.012	-7999.986

Table 11 - Comparison of a perfect dipole field harmonic analysis,  
 (a): uniform meshes of Table 9, and  
 (b): distorted meshes of Table 10.

TABLE FOR FIELD COEFFICIENTS

NORMALIZATION RADIUS = 2.00000

(a)

$$(BX - I BY) = I * \text{SUM } N * (AN + I BN) / R * (Z/R)^{**(N-1)}$$

N	N(AN)/R	N(BN)/R	ABS(N(CN)/R)	$b_n$	$a_n = 0$
1	8.0000E+03	0.0000E+00	8.0000E+03	$b_0 = 1.0$	
3	2.7857E-03	0.0000E+00	2.7857E-03	$b_3 = 0$	$b_1 = -7.8 \times 10^{-9}$
5	-4.8000E-03	0.0000E+00	4.8000E-03	$b_5 = 3.95 \times 10^{-10}$	
7	-3.0720E-04	0.0000E+00	3.0720E-04	$b_7 = 7.2 \times 10^{-10}$	
9	1.8537E-03	0.0000E+00	1.8537E-03	$b_9 = -9.0 \times 10^{-10}$	
11	-6.5911E-05	0.0000E+00	6.5911E-05	$b_{11} = 8.05 \times 10^{-11}$	
13	-1.4956E-04	0.0000E+00	1.4956E-04	$b_{13} = 4.57 \times 10^{-11}$	
15	-3.3133E-04	0.0000E+00	3.3133E-04	$b_{15} = 2.53 \times 10^{-11}$	
17	3.4713E-04	0.0000E+00	3.4713E-04	$b_{17} = -6.62 \times 10^{-12}$	

TABLE FOR FIELD COEFFICIENTS

NORMALIZATION RADIUS = 2.00000

(b)

$$(BX - I BY) = I * \text{SUM } N * (AN + I BN) / R * (Z/R)^{**(N-1)}$$

N	N(AN)/R	N(BN)/R	ABS(N(CN)/R)	$b_n$	$a_n = 0$
1	8.0000E+03	0.0000E+00	8.0000E+03		
3	1.1786E-03	0.0000E+00	1.1786E-03		<i>not calculated</i>
5	9.1429E-04	0.0000E+00	9.1429E-04		
7	2.8672E-03	0.0000E+00	2.8672E-03		
9	5.0556E-04	0.0000E+00	5.0556E-04		
11	-2.6364E-04	0.0000E+00	2.6364E-04		
13	1.9941E-04	0.0000E+00	1.9941E-04		
15	-2.2088E-04	0.0000E+00	2.2088E-04		
17	1.3351E-04	0.0000E+00	1.3351E-04		